From Differential Geometry of Curves to Helical Kinematics of Continuum Robots Using Exponential Mapping

Stanislao Grazioso$^{1(\boxtimes)}$, Giuseppe Di Gironimo^1, and Bruno Siciliano^2

^{1} Dipartimento di Ingegneria Industriale,
Università degli Studi di Napoli Federico II, P.le Tecchio 80, 80125 Napoli, Italy
{stanislao.grazioso,giuseppe.digironimo}@unina.it
^{2} Dipartimento di Ingegneria Elettrica e Tecnologie dell'Informazione,
Università degli Studi di Napoli Federico II, Via Claudio 21, 80125 Napoli, Italy
bruno.siciliano@unina.it

Abstract. Kinematic modeling of continuum robots is challenging due to the large deflections that these systems usually undergone. In this paper, we derive the kinematics of a continuum robot from the evolution of a three-dimensional curve in space. We obtain the spatial configuration of a continuum robot in terms of exponential coordinates based on Lie group theory. This kinematic framework turns out to handle robotic helical shapes, i.e. spatial configurations with constant curvature and torsion of the arm.

Keywords: Differential geometry · Continuum robotics · Kinematics

1 Introduction

The great capabilities for locomotion and manipulation exhibited by biological structures as elephant's trunks, snakes and octopus tentacle have inspired researchers towards recreating their robotics counterpart. A continuum (or continuous backbone) robot can be defined as a continuously bending, infinite degrees-of-freedom robot with an elastic structure [1]. The use of continuum robots in practical applications requires accurate mathematical models which can predict the robot's shape and motion. The inherent compliance of such mechanical systems suggests to use classical elasticity theories for long slender objects to describe their nonlinear behavior [2]. Despite recent improvements which have led to a faster computation of the governing equations for the robot's shape [3,4], we are still far to use these methods in real-time. Thus, over the years, a lot of effort has been done in deriving simplified and more analytically tractable models. A promising approach, mostly limited to kinematic analysis, begins by describing the desired three-dimensional curve in space, then fitting the physical robot to the theoretical analytical curve [5].

Using this approach, the constant curvature model have been developed [6]. It represent the robot as a series of mutually tangent circular arcs, which can be

described by only three parameters (radius of curvature, angle of the arc, bending plane). The constant curvature approximation has been successfully applied to many continuum robots [7,8]. However, this approach does not match the effective biological counterpart of novel designs, as the Festo's Bionic Handling Assistant (BHA), whose backbone curve has a continuously changing curvature [9]. The current variable curvature framework models the backbone of a single segment of the continuum manipulator using a piecewise constant curvature assumption. The major limit of current variable curvature kinematics framework is that they consider only bending and neglect torsion [10]. Hence, a variable curvature kinematic framework which can handle all the components of deformation is highly desirable.

In this paper, we derive a kinematic model for continuum manipulators using differential geometry techniques [11] and exponential coordinate representation [12], to provide an intuitive and effective description of the robot's configuration. The variable deformation framework is then integrated analitically under the hypothesis of constant curvature and torsion of the backbone. The shape of the robot turns out to possibly deform as a series of mutually tangent helixes, instead of circular arcs as in common variable curvature frameworks. We start by describing the evolution of a three-dimensional curve in space using the Serret-Frenet formulas. Then, we fit a continuum robot to the analytical curve through the exponential mapping. Finally, we give two examples and we demonstrate that this approach includes the constant curvature kinematics framework.

2   Geometric Description of a Spatial Curve

In classical differential geometry [11], a material abscissa $s \in [0,1]$ is usually used to parametrize a three-dimensional curve Γ. The position vector of a point $P \in \Gamma$ can be defined as $\boldsymbol{u}(s) = [u_1 \ u_2 \ u_3]^T$. The unit tangent vector is $\boldsymbol{t}(s) = \mathrm{d}\boldsymbol{u}(s)/\mathrm{d}s$, the unit normal vector $\boldsymbol{n}(s)$ is such that $\boldsymbol{t} \cdot \boldsymbol{n} = \boldsymbol{0}$, and the unit bi-normal vector $\boldsymbol{b}(s)$ is defined as $\boldsymbol{b} = \boldsymbol{t} \times \boldsymbol{n}$. The collection of these three unit vectors constitutes a local triad $\mathbf{R}(s) = [\boldsymbol{t}(s) \ \boldsymbol{n}(s) \ \boldsymbol{b}(s)]$ along the curve. The evolution of the curve in space is conveniently described by the formulas of Serret-Frenet [11], which take the form

$$\boldsymbol{t}'(s) = \kappa(s)\,\boldsymbol{n}(s) \tag{1}$$
$$\boldsymbol{n}'(s) = -\kappa(s)\boldsymbol{t}(s) + \tau(s)\boldsymbol{b}(s) \tag{2}$$
$$\boldsymbol{b}'(s) = -\tau(s)\boldsymbol{n}(s) \tag{3}$$

where $(\cdot)'$ denotes the derivative with respect to s, while $\kappa(s)$ and $\tau(s)$ indicate the curvature and the torsion of the curve. The vectors $\boldsymbol{t}'(s)$, $\boldsymbol{n}'(s)$, $\boldsymbol{b}'(s)$ can be collected in a 3×3 matrix $\mathbf{R}'(s) = [\boldsymbol{t}'(s) \ \boldsymbol{n}'(s) \ \boldsymbol{b}'(s)]$ such that the evolution of the curve in space can be written in the compact form (see e.g., Fig. 1)

$$\mathbf{H}'(s) = \mathcal{H}(\mathbf{R}'(s), \boldsymbol{u}'(s)) = \begin{bmatrix} \mathbf{R}'(s) & \boldsymbol{u}'(s) \\ \mathbf{0}_{1 \times 3} & 1 \end{bmatrix} \in SE(3) \tag{4}$$

where $SE(3)$ is the Special Euclidean group of the 4×4 homogeneous matrices.

Let us introduce a 4×4 matrix $\widetilde{\boldsymbol{f}}(s)$ as

$$\widetilde{\boldsymbol{f}}(s) = \begin{bmatrix} 0 & -f_{\omega_3}(s) & f_{\omega_2}(s) & f_{u_1}(s) \\ f_{\omega_3}(s) & 0 & -f_{\omega_1}(s) & f_{u_2}(s) \\ -f_{\omega_2}(s) & f_{\omega_1}(s) & 0 & f_{u_3}(s) \\ 0 & 0 & 0 & 0 \end{bmatrix} \in \mathfrak{se}(3) \tag{5}$$

where $\mathfrak{se}(3)$ is the Lie algebra associated to $SE(3)$. In screw theory, the elements of $\mathfrak{se}(3)$ are called twists. In this case, $\widetilde{\boldsymbol{f}}(s)$ takes the meaning of deformation twist of the curve. Notice that the Lie algebra $\mathfrak{se}(3)$ is isomorphic to $\mathbb{R}^6$, with $\boldsymbol{f}(s) = [\boldsymbol{f}_u^T(s) \ \boldsymbol{f}_\omega^T(s)]^T \in \mathbb{R}^6$.

With this in mind, Eq. 4 can be rewritten as

$$\mathbf{H}'(s) = \mathbf{H}(s)\widetilde{\boldsymbol{f}}(s) \tag{6}$$

stating that the spatial differential kinematics of the curve is simply expressed by the product of the deformation twist with the 4×4 homogeneous matrix

$$\mathbf{H}(s) = \mathcal{H}(\mathbf{R}(s), \boldsymbol{u}(s)) = \begin{bmatrix} \mathbf{R}(s) & \boldsymbol{u}(s) \\ \mathbf{0}_{1 \times 3} & 1 \end{bmatrix} \in SE(3) \tag{7}$$

which describe the configuration of the curve in three-dimensional space. Therefore, the current configuration of the curve in this variable deformation framework is computed by integrating (6) over the length of the curve, once that its deformation is known. This is not a trivial problem, since the three-dimensional curve evolves on $SE(3)$, which is a non-linear and non-commutative space. Indeed, closed-form solutions to (6) are usually unknown; general methods must employ a numerical integration scheme. Particularly appealing are the geometric integration schemes which do not involve parametrization of rotation, as the method of Crouch and Grossman [13] and the Munthe-Kaas [14]. In the next section we will provide an analytical solution to (6), which is appealing for describing the kinematics of a particular class of continuous backbone robots.
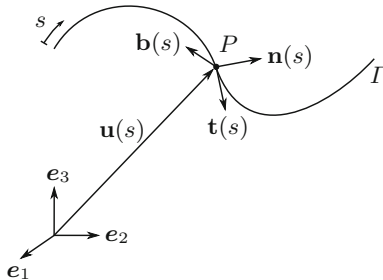

Fig. 1. Geometric description of a spatial curve.

3   Kinematic Modelling

Our kinematic approach is to fit the physical manipulator to the analytically desirable three-dimensional curve, whose evolution in space is described by (6). In this section we will derive a consistent helical kinematics framework which accounts for constant curvature and torsion of the robot's shape. Throughout this paper we will assume that the robot is inextensible and no shear effects are considered. With this hypothesis, the position and orientation parts of the deformation vector read

$$\boldsymbol{f}_u = \begin{bmatrix} 1 \\ 0 \\ 0 \end{bmatrix} \qquad \boldsymbol{f}_\omega = \begin{bmatrix} \tau \\ 0 \\ \kappa \end{bmatrix} \tag{8}$$

where we are considering initially straight configurations of the robot's shape aligned with $\boldsymbol{e}_1$ axis.

3.1   Forward Kinematics

Under the assumption of constant curvature and torsion, $\widetilde{\boldsymbol{f}}$ does not depend on s. Thus, the solution of (6) exists in closed form and it is given by

$$\mathbf{H}(s) = \mathbf{H}_0 \exp_{SE(3)}(s\boldsymbol{f}) \tag{9}$$

where $s \in [0, L]$, being L the length of the arm, $\mathbf{H}_0$, the configuration at $s = 0$, is a constant of integration, and $\exp_{SE(3)}(\cdot)$ is the exponential mapping on $SE(3)$, which maps an element of the Lie algebra $\widetilde{\boldsymbol{f}} \in \mathfrak{se}(3)$ into an element of the Lie group $\mathbf{H} \in SE(3)$. Formally, it is defined by

$$\exp_{SE(3)}(\boldsymbol{f}) = \begin{bmatrix} \exp_{SO(3)}(\boldsymbol{f}_\omega) & \mathbf{T}_{SO(3)}^T(\boldsymbol{f}_\omega)\boldsymbol{f}_u \\ \mathbf{0}_{1\times 3} & 1 \end{bmatrix} \tag{10}$$

where $\exp_{SO(3)}(\cdot)$ is the exponential map on the special Orthogonal group $SO(3)$, the group of the rotation matrices. This is given by

$$\exp_{SO(3)}(\boldsymbol{f}_\omega) = \mathbf{I}_{3\times 3} + \alpha(\boldsymbol{f}_\omega)\widetilde{\boldsymbol{f}}_\omega + \frac{\beta(\boldsymbol{f}_\omega)}{2}\widetilde{\boldsymbol{f}}_\omega^2 \tag{11}$$

and it is known as Rodrigues' formula. In (11), we have

$$\alpha(\boldsymbol{f}_\omega) = \frac{\sin(\|\boldsymbol{f}_\omega\|)}{\|\boldsymbol{f}_\omega\|} \qquad \beta(\boldsymbol{f}_\omega) = 2\frac{1 - \cos(\|\boldsymbol{f}_\omega\|)}{\|\boldsymbol{f}_\omega\|^2} \tag{12}$$

Indeed, $\mathbf{T}_{SO(3)}^T(\cdot)$ is the transpose of the tangent operator on $SO(3)$, which is defined from the derivative of the exponential map as

$$\mathbf{T}_{SO(3)}(\boldsymbol{f}_\omega) = \mathbf{I}_{3\times 3} - \frac{\beta(\boldsymbol{f}_\omega)}{2}\widetilde{\boldsymbol{f}}_\omega + \frac{1 - \alpha(\boldsymbol{f}_\omega)}{\|\boldsymbol{f}_\omega\|^2}\widetilde{\boldsymbol{f}}_\omega^2 \tag{13}$$

By separating the rotation and position part of (9), we obtain

$$\mathbf{R}(s) = \mathbf{R}_0 \exp_{SO(3)}(s\boldsymbol{f}_\omega) \tag{14}$$

$$\boldsymbol{u}(s) = \boldsymbol{u}_0 + \mathbf{R}_0 \mathbf{T}_{SO(3)}^T (s\boldsymbol{f}_\omega) \, s\boldsymbol{f}_u \tag{15}$$

where $\mathbf{R}_0$, the rotation matrix at $s = 0$, and $\boldsymbol{u}_0$, the position vector at $s = 0$, are constant of integration. Since we are considering arms aligned with $\boldsymbol{e}_1$ and initially straight, we have $\mathbf{R}_0 = \mathbf{I}_{3\times3}$ and $\boldsymbol{u}_0 = \mathbf{0}_{3\times1}$.

As a matter of fact, the exponential mapping introduces a local parametrization which allows describing the configuration of a curve, which belongs to $SE(3)$, i.e. a non-commutative and non-linear space, with an element belonging to a linear space, namely the Lie algebra $\mathfrak{se}(3)$.

3.2   Inverse Kinematics

The inverse kinematics maps the configuration of the continuum robot to the deformation vector. In our hypothesis, the inversion of (9) exists in closed form and it is given by

$$\boldsymbol{f} = \log_{SE(3)}\left(\mathbf{H}_0^{-1}\mathbf{H}_L\right) \tag{16}$$

where $\mathbf{H}_L$ is the configuration at $s = L$, and $\log_{SE(3)}(\cdot)$ is the logarithmic mapping on $SE(3)$, which maps back an element of the Lie group into an element of its corresponding Lie algebra. It is defined by

$$\log_{SE(3)}(\mathbf{H}) = \begin{bmatrix} \widetilde{\boldsymbol{f}}_\omega & \mathbf{T}_{SO(3)}^{-T}(\boldsymbol{f}_\omega)\boldsymbol{u} \\ \mathbf{0}_{1\times3} & 1 \end{bmatrix} \tag{17}$$

where we have indicated $\mathbf{H} = \left(\mathbf{H}_0^{-1}\mathbf{H}_L\right)$, $\widetilde{\boldsymbol{f}}_\omega = \log_{SO(3)}(\mathbf{R})$ and

$$\log_{SO(3)}(\mathbf{R}) = \frac{\theta}{2\sin\theta}(\mathbf{R} - \mathbf{R}^T) \tag{18}$$

with

$$\theta = \mathrm{acos}\left(\frac{1}{2}(\mathrm{trace}(\mathbf{R}) - 1)\right), \qquad \theta < \pi \tag{19}$$

Indeed, $\mathbf{T}_{SO(3)}^{-T}(\cdot)$ is the transpose of the inverse of the tangent operator on $SO(3)$, which is defined as

$$\mathbf{T}_{SO(3)}^{-1}(\boldsymbol{f}_\omega) = \mathbf{I}_{3\times3} + \frac{1}{2}\widetilde{\boldsymbol{f}}_\omega + \frac{1 - \gamma(\boldsymbol{f}_\omega)}{\|\boldsymbol{f}_\omega\|^2}\widetilde{\boldsymbol{f}}_\omega^2 \tag{20}$$

with

$$\gamma(\boldsymbol{f}_\omega) = \frac{\|\boldsymbol{f}_\omega\|}{2}\cot\left(\frac{\|\boldsymbol{f}_\omega\|}{2}\right) \tag{21}$$

4   Test Cases

In this section we consider two test examples, one relating a continuum arm with constant curvature, one relating a continuum arm with constant curvature and torsion.

4.1   Continuum Arm with Constant Curvature

Let $\boldsymbol{f}_\omega = [0 \ 0 \ \kappa]^T$. By developing (9), it is easy to demonstrate that the configuration of the robotic arm is given by

$$\mathbf{H}(s) = \begin{bmatrix} \cos(s\kappa) & -\sin(s\kappa) & 0 & \frac{1}{\kappa}\sin(s\kappa) \\ \sin(s\kappa) & \cos(s\kappa) & 0 & \frac{1}{\kappa}(1 - \cos(s\kappa)) \\ 0 & 0 & 1 & 0 \\ 0 & 0 & 0 & 1 \end{bmatrix} \tag{22}$$

which corresponds to the robot's shape obtained with constant curvature kinematics framework [6,15]. A circular desired end point trajectory is shown in Fig. 2. The parameters used in this example are: $L = 1$m; $\kappa = \pi/10 : \pi/10 : \pi$m^{-1}.

It is easy to verify that, computing $\mathbf{H}_0 = \mathbf{H}(s = 0)$ and $\mathbf{H}_L = \mathbf{H}(s = L)$ from (22), the use of (17) gives back $\boldsymbol{f}_\omega = [0 \ 0 \ \kappa]^T$.
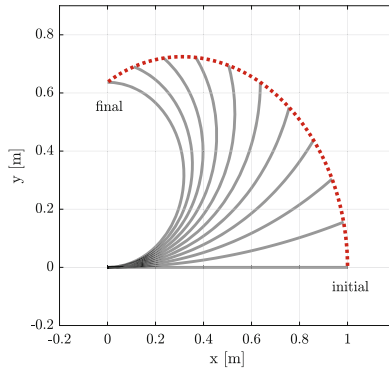

Fig. 2. Whole arm shape configuration under a desired circular end point trajectory.

4.2   Continuum Arm with Constant Curvature and Torsion

Let $\boldsymbol{f}_\omega = [\tau \ 0 \ \kappa]^T$. By developing (9), the configuration of the robotic arm is given by

$$\mathbf{H}(s) = \begin{bmatrix} 1 - (1 - \cos(s\kappa_g))\frac{\kappa^2}{\kappa_g^2} & -\sin(s\kappa_g)\frac{\kappa}{\kappa_g} & (1 - \cos(s\kappa_g))\frac{\kappa\tau}{\kappa_g^2} & s + (\sin(s\kappa_g) - s\kappa_g)\frac{\kappa^2}{\kappa_g^3} \\ \sin(s\kappa_g)\frac{\kappa}{\kappa_g} & \cos(s\kappa_g) & -\sin(s\kappa_g)\frac{\tau}{\kappa_g} & (1 - \cos(s\kappa_g))\frac{\kappa}{\kappa_g^2} \\ (1 - \cos(s\kappa_g))\frac{\kappa\tau}{\kappa_g^2} & \sin(s\kappa_g)\frac{\tau}{\kappa_g} & 1 - (1 - \cos(s\kappa_g))\frac{\tau^2}{\kappa_g^2} & (s\kappa_g - \sin(s\kappa_g))\frac{\kappa\tau}{\kappa_g^3} \\ 0 & 0 & 0 & 1 \end{bmatrix} \tag{23}$$

where $\kappa_g = \sqrt{\kappa^2 + \tau^2}$ is the Gaussian curvature of the arm. Equation (23) correspond to an helical-shaped configuration of the whole arm. Figure 3 illustrate a typical screw motion. The left hand figure shows the motion corresponding to a fixed torsion $\tau = 3\,\mathrm{m}^{-1}$ and varying curvature $\kappa = 0 : \pi/2 : 2\pi\,\mathrm{m}^{-1}$. Indeed, the right hand figure shows the motion corresponding to a fixed curvature $\kappa = 3\,\mathrm{m}^{-1}$ and varying torsion $\tau = 0 : \pi/2 : 2\pi\,\mathrm{m}^{-1}$.

It is easy to verify that, again, computing $\mathbf{H}_0 = \mathbf{H}(s = 0)$ and $\mathbf{H}_L = \mathbf{H}(s = L)$ from (23), the use of (17) gives back $\boldsymbol{f}_\omega = [\tau\ \ 0\ \ \kappa]^T$.
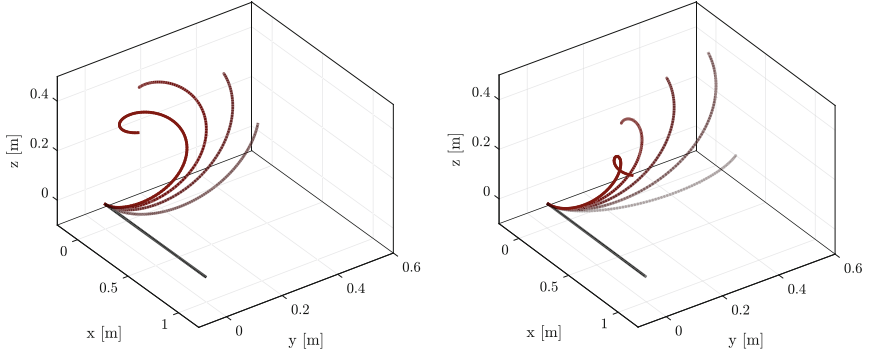

Fig. 3. Whole arm screw motion of a manipulator with constant curvature and torsion.

5   Conclusions

A variable deformation kinematic framework based on differential geometry has been presented for spatial three-dimensional curves. In order to derive analytical solutions, we have integrated the spatial differential kinematic model by using a constant deformation assumption. In particular, we have developed the analytical solutions for constant curvature and torsion robots, whose backbone configuration in space resembles the shape of an helix, i.e. a spatial curve with constant curvature and torsion.

The kinematic modeling of compound continuum robots will arise naturally from the framework. Future works of the authors will investigate closed-loop inverse kinematics algorithms to iteratively solve the inverse kinematics of single-segment and multiple-segments continuum robots.

References

1. Walker, I.D., Choset, H., Chirikjian, G.S.: Snake-like and continuum robots. In: Springer Handbook of Robotics, pp. 481–498. Springer, Cham (2016)
2. Simo, J.C., Vu-Quoc, L.: A three-dimensional finite-strain rod model. part II: Computational aspects. Comput. Methods Appl. Mech. Eng. **58**(1), 79–116 (1986)
3. Grazioso, S., Sonneville, V., Di Gironimo, G., Bauchau, O., Siciliano, B.: A nonlinear finite element formalism for modelling flexible and soft manipulators. In: 2016 IEEE International Conference on Simulation, Modeling, and Programming for Autonomous Robots, pp. 185–190. IEEE (2016)
4. Grazioso, S., Di Gironimo, G., Siciliano, B.: A geometrically exact model for soft robots: the finite element deformation space formulation. Soft Robotics
5. Andersson, S.B.: Discretization of a continuous curve. IEEE Trans. Rob. **24**(2), 456–461 (2008)
6. Webster III, R.J., Jones, B.A.: Design and kinematic modeling of constant curvature continuum robots: a review. Int. J. Rob. Res. **29**(13), 1661–1683 (2010)
7. Hannan, M.W., Walker, I.D.: Kinematics and the implementation of an elephant's trunk manipulator and other continuum style robots. J. Field Rob. **20**(2), 45–63 (2003)
8. Jones, B.A., Walker, I.D.: Kinematics for multisection continuum robots. IEEE Trans. Rob. **22**(1), 43–55 (2006)
9. Grzesiak, A., Becker, R., Verl, A.: The bionic handling assistant: a success story of additive manufacturing. Assem. Autom. **31**(4), 329–333 (2011)
10. Mahl, T., Hildebrandt, A., Sawodny, O.: A variable curvature continuum kinematics for kinematic control of the bionic handling assistant. IEEE Trans. Rob. **30**(4), 935–949 (2014)
11. Struik, D.J.: Lectures on classical differential geometry. Courier Corporation, North Chelmsford (2012)
12. Lynch, K.M., Park, F.C.: Modern Robotics: Mechanics, Planning, and Control. Cambridge University Press, Cambridge (2017)
13. Crouch, P.E., Grossman, R.: Numerical integration of ordinary differential equations on manifolds. J. Nonlinear Sci. **3**(1), 1–33 (1993)
14. Munthe-Kaas, H.: Runge-Kutta methods on lie groups. BIT Numer. Math. **38**(1), 92–111 (1998)
15. Grazioso, S., Di Gironimo, G., Siciliano, B.: Analytic solutions for the static equilibrium configurations of externally loaded cantilever soft robotic arms. In: 2018 IEEE International Conference on Soft Robotics. IEEE (2018)